Fisheries Oceanography
Volume 15 Issue 5 Page 413 - September 2006
http://dx.doi.org/10.1111/j.1365-2419.2006.00409.x

One-dimensional biophysical modelling of fish egg vertical distributions in shelf seas

Pierre Petitgas [1,*], Stéphanie Magri [2] and Pascal Lazure [2]

[1] IFREMER, BP 21105, F- 44311 cedex 03, Nantes, France.
[2] IFREMER, BP 70, F-29280, Plouzané, France.

[*] Correspondence:
phone: +33 240 374163
fax: +33 240 374075
e-mail: Pierre.Petitgas@ifremer.fr.

Abstract:

Modelling the vertical distribution of fish eggs is important when assessing fish stocks with egg production methods and for monitoring the reproductive potential of fish populations. Fish eggs are passive particles and their vertical distribution is determined by a few parameters such as egg density, egg diameter, wind- and tide-induced turbulence, and vertical hydrographic structure. A one-dimensional vertical biophysical, numerical model was developed which was adapted to the hydrography of shelf seas under the influence of tidal currents, wind-induced circulation, and river discharges. The biological part of the model parameterized the ascent velocity of the egg as a function of egg properties (diameter, density) and water properties (density, viscosity, turbulence). The model contains a turbulence closure which makes the model dynamic. The model parameters were surface wind, tidal currents, T-S profile, and egg diameter and density, which were kept constant in time. The model has the capacity to generate sub-surface egg maxima in different hydrographic conditions, e.g. in areas under the influence of river plumes, and can also homogenize the egg distribution under wind and tide forcing. Sensitivity tests were carried out to study the response of the model to variations in the model parameters for a variety of hydrographic conditions. The modelled egg vertical distributions were validated by comparison of the model results with egg distributions sampled in the field. The analysis highlighted variability in fish egg density of anchovy, sardine, and sprat across years and areas, with a potential link between egg density and surface sea water density. The validated model is a tool for the analysis of shelf seas fish egg vertical distributions.

Key words: Bio-physical coupling, Fish egg buoyancy, Vertical distribution, CUFES

INTRODUCTION

Knowledge of the vertical distribution of fish eggs and larvae is central for several aspects of fisheries science, such as understanding recruitment processes, monitoring stocks with egg production methods and sampling ichthyoplankton. The vertical distribution of eggs and larvae is essential for understanding how horizontal drift (e.g., Heath et al., 1991; Stenevik et al., 2001; Parada et al., 2003), food availability (e.g., Palomera et al., 1991; Conway et al., 1997) and habitat variability (e.g., Nissling and Vallin, 1996) affect ichthyoplankton survival and potentially recruitment. It is also of prior importance for estimating ambient developmental temperature of fish eggs when evaluating fish stocks using egg surveys (e.g., Zeldis et al., 1995; Motos and Coombs, 2000; Coombs et al., 2001) and is a prerequisite for efficient quantitative sampling of the ichthyoplankton at sea (e.g., Moser and Pommeranz, 1999). Modelling the vertical distribution of fish eggs has been recently revived (Boyra et al., 2003) because of the development of the egg pump CUFES (continuous underway fish egg sampler, Checkley et al., 1997). This instrument operates at 3m depth and is potentially useful in egg surveys (Checkley at al., 2000; Lo et al., 2001) and can be used together with acoustics to detect adult spawning fish (Petitgas et al., 2002).

The vertical distribution of pelagic eggs is determined by a set of interacting biological and physical processes (Sundby, 1991), namely the properties of the eggs (density, diameter) and the ambient sea water (density, viscosity, turbulence). Two models for predicting the egg vertical distribution have been developed (Sundby, 1983; Westgard, 1989). Sundby (1983) proposed for a homogeneous wind mixed layer an analytic steady-state solution which balances the egg ascent velocity with the wind induced turbulence. Westgard (1989) proposed a dynamic numerical model with a two level turbulence closure scheme to account for depth-varying turbulent diffusion. This approach allowed him to analyse transient egg distributions through time as well as steady-state distributions. The model of Sundby (1983) was successfully applied in open ocean areas where the hypotheses of homogeneous turbulent diffusion in the mixed layer was relevant (Sundby, 1983; Ådlandsvik et al., 2001; Stenevik et al., 2001). This assumption was relaxed to account for given parametric formulations of depth varying turbulence in order to model sub-surface peaks in the egg distribution but with varying success (Tanaka, 1992; Boyra et al., 2003). In contrast, the numerical model of Westgard (1989) accomodates a variety of hydrodynamic conditions including situations where haline stratification of the water column generates complex depth variation in turbulent diffusion.

On the French shelf in the Bay of Biscay, pelagic fish stocks (engraulid and clupeoid) and the pelagic ecosystem are monitored in spring by fisheries acoustic surveys, with particular focus on anchovy and sardine. During the surveys the CUFES egg pump is operated together with the acoustics allowing for the cross-validation of assessment methods and the study of the ecology of spawning grounds. For these purposes the pumped 3m depth egg concentration needs to be converted to a vertically integrated egg abundance. Such conversion requires modelling the egg vertical distribution. During spring,

hydrographic conditions are diverse on the French Biscay shelf (as observed in the surveys) with water column stratification being due to salinity or temperature or both and with turbulent diffusion being due to wind and tide (Planque et al., 2003).

The object of the present paper was to develop further the numerical model of Westgard (1989) to incorporate tidal forcing and develop a frame work for modelling vertical egg distributions in shelf seas including areas under the influence of tide and river plumes. The model sensitivity to input parameters (wind, tide, egg density and diameter) was analysed in a variety of hydrographic situations typical of the Biscay French shelf. The model was then validated by comparing its outputs with published *in situ* vertical distributions selected from the literature. It appeared that egg density could vary from year to year depending on surface hydrographic conditions.

MATERIALS AND METHODS

The one-dimensional vertical model

The physical model

The hydrodynamic model is a one-dimensional dynamical and numerical model forced by wind and tide. In order to simulate tidal effects, free surface elevation gradients are considered. The model has five state variables, namely temperature, salinity, velocities (u,v) and turbulence kinetic energy. The turbulence closure is achieved by an algebraic formulation of the mixing length.

The two components of the velocity were:

$$\begin{cases} \dfrac{\partial u}{\partial t} - fv = -g\dfrac{\partial \xi}{\partial x} + \dfrac{\partial}{\partial z}\left(n_z \dfrac{\partial u}{\partial z}\right) & (1) \\ \dfrac{\partial v}{\partial t} + fu = -g\dfrac{\partial \xi}{\partial y} + \dfrac{\partial}{\partial z}\left(n_z \dfrac{\partial v}{\partial z}\right) & (2) \end{cases}$$

with the following notations:

t: time

z: vertical coordinate (positive upward)

u: E-W velocity (m s^{-1})

v: N-S velocity (m s^{-1})

g: gravitational acceleration (9.81 m s^{-2})

f: Coriolis parameter (10^{-4} s^{-1})

n_z: vertical eddy viscosity (m^2 s^{-1})

$\left(\dfrac{\partial \xi}{\partial x}, \dfrac{\partial \xi}{\partial y}\right)$: free surface elevation gradient

The surface condition was:

$$n_z\left(\frac{\partial u}{\partial z}, \frac{\partial v}{\partial z}\right) = \left(\frac{\tau_x}{\rho}, \frac{\tau_y}{\rho}\right)$$

with the following notations:

$\left(\dfrac{\tau_x}{\rho}, \dfrac{\tau_y}{\rho}\right)$: surface wind stress components

ρ: density of sea water (kg m^{-3})

The bottom condition was:

$$n_z\left(\frac{\partial u}{\partial z}, \frac{\partial v}{\partial z}\right) = C_d \sqrt{{u_b}^2 + {v_b}^2}\,(u_b, v_b)$$

where C_d is the drag coefficient ($2.5\ 10^{-3}$) and u_b,v_b the velocities in the bottom layer.

For the tidal forcing, we applied the linear theory of tide that indicates that the horizontal gradient induced by a tidal wave propagating in one direction can be expressed as the following horizontal gradient:

$$\left(\frac{\partial \xi}{\partial x}, \frac{\partial \xi}{\partial y}\right) = \frac{U_0}{gT}\left(\cos(2\pi t/T), \sin(2\pi t/T)\right)$$

with the following notations:

T: M_2 tidal period (44712s)

U_0: the maximum tidal current reached during a tidal cycle

The turbulence closure model was based on the turbulence kinetic energy (TKE) state equation and an algebraic formulation of the mixing length (Luyten et al, 1996):

$$\frac{\partial k}{\partial t} = \frac{\partial}{\partial z}\left(n_z \frac{\partial k}{\partial z}\right) + P_s + G - \varepsilon$$

with the following notations:

k: turbulent kinetic energy (TKE : $m^2\ s^{-2}$)

ε: dissipation rate of TKE ($m^{-2}\ s^{-3}$)

P_s: production of TKE by vertical velocity gradient: $P_s = n_z\left(\left(\frac{\partial u}{\partial z}\right)^2 + \left(\frac{\partial v}{\partial z}\right)^2\right)$

G: reduction of TKE by vertical density gradient: $G = -gk_z \frac{1}{\rho}\frac{\partial \rho}{\partial z}$

k_z: vertical eddy diffusivity ($m^2\ s^{-1}$)

In the present one-equation turbulence closure scheme, ε is given by a function of TKE and the mixing length l:

$\varepsilon = \varepsilon_0 \frac{k^{3/2}}{l}$, where ε_0 =0.166 and $l_z = \kappa z(1 - z/H)^{1/2}$ with the Karman constant $\kappa = 0.4$

Finally, turbulent eddy viscosity and eddy diffusivity are given by:

$n_z = S_u k^2/\varepsilon$ and $k_z = S_b k^2/\varepsilon$

Where S_u and S_b are stability functions which expressions can be found in Luyten et al. (1996).

Though similar to that of Westgard (1989), our model differs from it in two ways. In our model, (i) tidal current is taken into account (which was not the case in Westgard, 1989) and (ii) ε is estimated as a function of the mixing length (we have a one equation k closure scheme and not a two equation k-ε closure scheme as in Westgard, 1989). Luyten et al. (1996) compared different turbulence closure schemes for shelf stratified waters and concluded that there was no difference in the results between the two schemes, the k closure scheme being less computer intensive.

Being dynamical and numerical, the model can be applied in situations with homogeneous or stratified vertical profiles of temperature and salinity and in particular it can accommodate any type of

gradient in turbulent eddy diffusivity due to complex haloclines on the shelf under the influence of river plumes. The model can also estimate the steady-state vertical distribution as well as a time-dependent distribution depending on the duration of the simulation in relation to that of the egg stages.

The coupled biological model

The hydrodynamic model is coupled with a biological model which parameterises the ascent velocity of fish eggs. The state equation of the egg concentration is:

$$\frac{\partial \varphi}{\partial t} = \frac{\partial}{\partial z}\left(k_z \frac{\partial \varphi}{\partial z}\right) - \frac{\partial w \varphi}{\partial z} \quad (3)$$

where φ is the egg concentration (no eggs m^{-3}), w the egg ascent terminal velocity (m s^{-1}), k_z the eddy diffusivity (m^2 s^{-1}). The vertical egg distribution φ thus results from the interaction between turbulent mixing as given by k_z and advection as given by w, where k_z and w are estimated by the physical and the biological parts of the model.

The ascent velocity w depends on the egg diameter d, the density difference $\Delta\rho$ (kg m^{-3}) between the egg and the ambient sea water and the viscosity μ of the sea water. The parameterisation of w is given by Stokes' law or Dalavalle's law depending on the value of the Reynolds number (Dalavalle, 1948; Hutchinson, 1967; Sundby, 1983). The switch to Dalavalle's parametrisation from Stokes' law with increasing Reynolds number has the consequence to lower the ascent velocity of the egg when sea water becomes less viscous and more turbulent. When the Reynolds number $Re = \rho_{water}\, w\, d / \mu$ is smaller than 0.5, viscosity forces dominate over frictional forces and w is given by Stokes's law:

$$w = \frac{g\, d^2\, \Delta\rho}{18\, \mu}$$

where μ is the dynamic viscosity (kg m^{-1} s^{-1}) which depends on temperature and salinity (Table 1). When the Reynolds number is greater than 0.5, viscosity forces decrease in importance because of an increase in turbulence and in that case w is given by the equation of Dalavalle (1948):

$$w = \frac{K_I d_0 \Delta\rho^{2/3}}{\mu^{1/3}}$$

where K_I is a constant equal to 0.088 in SI units (19 in cgs units: Sundby, 1983) and d_o is given by Sundby (1983):

$$d_0 = d - c\,D = d - c\left(\frac{9\,\mu^2}{\rho_{egg}\, g\, \Delta\rho}\right)^{1/3}$$

with D is the uppermost limit of egg size to which the Stokes equation applies and c a constant equal to 0.4 for spheres.

We used this two regime settling velocity scheme following fisheries litterature (e.g., Sundby, 1983) although formulations have been proposed with continuous functions of Reynolds number that implicitly allow for the transition from low to high Reynolds numbers and that are not dependent on a calibration constant (e.g., Denny, 1993; Clift et al., 1978).

Model implementation

Model numerical solving scheme

Equations 1 and 2 are discretized on the vertical on a staggered grid: n_z, k_z are calculated between the points at which are calculated u, v and φ. Equations 1 and 2 are not solved at the same time but alternatively every half time step to obtain a temporally centered scheme for the Coriolis force. Variables φ, TKE, n_z and k_z are calculated every time step. All vertical derivatives are considered as implicit which leads to a three diagonal matrix solved by standard method, including near surface and bottom.

Model application

The vertical grid mesh size was 1 m. The maximum tidal amplitude, U_0, varies in space and was set as a local condition as for Coriolis parameter, f, and water depth, H. Values of U_0 for the Bay of Biscay and English Channel are calculated by a general 2D tidal model, which gives similar results to earlier calculations of Pingree et al. (1982) and Le Cann (1990). Sea water density profile (derived from the vertical temperature and salinity profiles), wind speed, tidal amplitude U_0, egg diameter and density were kept constant during the whole simulation.

Characteristic time and initial condition

The steady-state egg distribution was obtained by the balance between turbulent mixing and egg migration as formulated in equation (3). The characteristic time was derived from the dimension analysis of equation (3). The egg migration time scale, $H / \overline{w}$, is the time necessary for the egg to attain a steady-state distribution starting from a homogeneous initial egg distribution by advection only. The physical mixing time scale, $H^2 / \overline{k}_z$, is the time necessary to attain a steady-state by vertical mixing only. The relevant characteristic time is the smallest of these two time scales and determines if the steady-state is attained because of physical mixing or egg migration. If the characteristic time is smaller than the egg life span duration, the egg can attain its steady-state distribution. The *in situ* distribution is then independent of the initial condition and can be estimated with the steady-state solution of the model. In contrast, if the characteristic time is greater than the egg life span duration, the egg cannot attain a steady-state. In that case, the *in situ* egg distribution will depend on the initial condition of spawning and can only be estimated by a transient solution of the model. All simulations

were performed for 20 days starting from a homogeneous vertical distribution, which was a sufficiently long time for the modelled egg distribution to attain a steady-state in all the considered cases. The characteristic time was estimated at the beginning of each simulation. Each simulation was initialised with a homogeneous egg distribution and $\overline{w}$ was estimated using the coresponding initial values of w. For estimating $\overline{k}_z$ we used the values k_z after the first tidal cycle. The first tidal cycle allowed for n_z, k_z, and TKE to stabilize starting from their initial values (respectively 10^{-4}, 10^{-4} and 0).

Model sensitivity

The response of modelled egg distributions (model ouputs) to physical and biological parameter variation (model inputs) was analysed for typical spring-time Bay of Biscay hydrological situations and for anchovy and sardine. Four input parameters were retained: wind, tide, egg diameter and egg density.

Spring-time (May-June) fisheries acoustic surveys of IFREMER provided temperature and salinity profiles at CTD stations covering the entire French shelf of the bay of Biscay (2000-2003). The hydrological profiles where characterised using four variables following Planque et al. (2003): surface temperature and salinity, bottom temperature, depth of maximum density gradient. A hierarchical clustering of all CTD stations was performed. Four hydrological groups were identified: group G1 was characterised by a small density gradient, group G2 by a haline gradient, group G3 by a temperature gradient and group G4 by both haline and temperature gradients (Table 2, Fig. 1). In each group, the station closest to the group centre was selected to represent the group. These stations were used as reference stations in the sensitivity analysis with their hydrological structure, wind and tide conditions.

A reference run (RR) was performed at each reference station using the parameters compiled in Tables 2 and 3: observed wind at reference station, tidal current of 0.8 m s^{-1} corresponding to an average value for Biscay, the Celtic Sea and the English Channel, average egg diameter and density reported by Coombs et al. (2004) and Boyra et al. (2003). Then each parameter (wind, tide, egg diameter and density) was varied one at a time, the other parameters being kept at their reference value. For each run and each hydrological condition, the root mean square difference (RMSD) between the estimated egg distribution and that of the RR was computed over the first 50 m. The egg concentration φ was expressed as the percentage at depth of total egg abundance in the water column. RMDS values allowed us to quantify the impact on the egg distribution of each input parameter in each hydrological condition, compare the impact between parameters in each hydrological condition and compare the impact for each parameter across the hydrological conditions. Another metric was used to describe in detail egg concentrations in the upper 5 m of the vertical distribution. This metric was the percent increase or decrease of eggs in the first 5 m relative to the egg abundance of the RR in those first 5 m.

Model validation

The model was validated using published *in situ* egg vertical distributions sampled with the Longhurst-Hardy Plankton Recorder (LHPR, Williams et al., 1983). At each of the LHPR sampling stations, the following parameters were necessary to run the model: geographical position and date, temperature and salinity profiles, wind speed, tidal current, egg diameter and density. Published material was selected based on the availability of this set of parameters in the articles as well as on the processes to be validated. The biological part of the model was validated using deep egg distributions of blue whiting that were below the depth of wind induced turbulence (Adlansvik et al., 2001). The model dynamics in the presence of wind and tide was validated using egg distributions of sardine and sprat in the Channel in summer with thermal stratification as well as in autumn with homogeneous water column structure (Coombs et al., 1985). The model dynamics in the presence of wind, tide, thermal and haline stratifications were validated using egg distributions of anchovy and sardine in Biscay in spring (Motos and Coombs, 2000; Coombs et al., 2004). Stations were selected that showed a surface peak, a sub-surface peak and a deep peak in the egg distribution. T-S and egg profiles were scanned from the published figures and interpolated at 1 m interval for comparison with the vertical model output. Egg density in the model was varied to produce best fit between modelled and observed vertical distributions. The fitted egg density was then compared to available published measurements performed with the density-gradient column of Coombs (1981). In each validation experiment, the egg characteristic time was estimated. Except for the blue whiting for which initial conditions were provided, in all other cases the model initial egg distribution was homogeneous: at each depth, the egg concentration was equal to the total number of eggs counted from bottom to surface at the station divided by depth (grid mesh size being 1 m). The homogeneous initial distribution was equivalent to assuming that eggs were spawned in equal amounts at all depths.

RESULTS

Sensitivity analysis

In this section we assess the responses of modelled egg distributions to varying egg shape, density and hydrographic forcing.

Impact of anchovy egg shape

The egg of sardine is spherical but the egg of anchovy is a prolate ellipsoid. As Stokes' law applies for spheres, the anchovy egg ascent velocity may depart from that calculated with Stokes' law. Hutchinson (1967, Fig.75 p.262) provides corrections from Stokes' law for an ellipsoid as a function of the ratio between ellipsoid axes and the orientation of the ellipsoid during its motion. Coombs et al. (2004) report that the mean egg diameter for anchovy in Biscay was 0.7 mm x 1.5 mm (the sphere of equivalent volume having a diameter of 0.89 mm) and that the orientation of anchovy eggs was along their long axis during measurements in the density-gradient column (the embryo effectively develops at one pole of the egg). In this situation, the ascending velocity of the egg would be 0.96 that of its equivalent sphere (Hutchinson, 1967). This small correction on the egg velocity had no impact on the egg distribution. Anchovy eggs were therefore considered as spheres of equivalent volume, an approach followed by Coombs et al. (2004) for anchovy and Ådlandsvik et al. (2001) for blue whiting larvae.

Sensitivity in the first 50 m

From the structure of the model, it is expected that increasing wind will increase mixing from the surface down through the water column, that increasing tide will increase mixing from the bottom upwards, both resulting in homogenising the egg distribution. Increasing egg size is expected to increase ascent egg velocity and reduce the time scale to attain steady-state. In contrast, increasing egg density is less easily predictable as its effect depends on the sea water density profile. Variation in the input parameters for the sensitivity analysis is compiled in Table 3. The RMSD values (Table 4) showed wind to have an important impact in all hydrological groups and in particular, low wind condition changed radically the egg distribution in group G4. Tide had no effect except in coastal group G2. It is then expected that in coastal waters the spring-neap tidal cycle has a significant effect on the vertical egg distribution. Egg diameter had no impact in groups G1 and G3 but a small one in groups G2 for anchovy and G4 for both anchovy and sardine. Impact of egg density was similar except that it was very important in groups G2 and G4.

Situations with high RMSD values were analysed further by examining the egg vertical profiles (Figs 2-5). Low wind condition at station G4 (Fig. 2) allowed the anchovy eggs to concentrate in a pronounced sub-surface peak (7 m depth) which corresponded to the depth of neutral buoyancy. The peak was present in the RR but smoothed in the stronger wind condition, which agreed with the

vertical profile of TKE (Fig. 2). Low tidal current at station G2 (Fig. 3) allowed anchovy eggs to concentrate at the surface (0-5 m), which was prevented by stronger tidal currents as shown by the profile of turbulence (Fig. 3). Increasing anchovy egg density at station G2 (Fig. 4) generated a deep peak (13 m) which corresponded to the depth of neutral egg buoyancy for that density. In contrast, with a lower density value, the egg showed an upward velocity at all depths and the maximum egg concentration was in the surface layer (0-5 m). Larger sardine egg density at station G2 (Fig. 5) also generated deep peaks (7 m and 13 m) which corresponded to the depths of neutral buoyancy for these densities. As in the anchovy case, with a lower density value the maximum egg concentration was in the surface layer (0-5 m). In the experiments on varying egg density at station G2 (Figs. 4 and 5), both wind and tide were of small amplitude (Table 2) leading to little turbulent mixing and allowing the egg to attain its depth of neutral buoyancy. Similar effects of varying wind and egg density occurred at station G4 for both anchovy and sardine but were less pronounced (not shown). Sardine and anchovy egg profiles were more sentitive to variations in the egg density in the case of complex hydrological structures such as G2 and G4 (typical of the shelf) in comparison to conditions G1 and G3 (more typical of oceanic conditions).

Sensitivity in the first 5 m.

The impact of variations in the input parameters was further assessed for the CUFES which is a surface pumping device (at 3 m): we estimated the resulting variation in the surface (0-5 m) egg concentration relatively to that of the RR (Table 5). High variations in this layer occurred in the cases where RMSD was large (Table 4) but also in other cases. Variation in this layer was sensitive in nearly all parameters and hydrological conditions, except for tide in groups G1 and G3, anchovy diameter in group G2 and sardine density in groups G1 and G3. RMSD quantified overall variation in the profile shape (50 values used) when the focus was only on 5 values of egg concentration at the surface. This means that CUFES samples are expected to have high variability and that a precise estimate of the water column egg integral using the model will require accurate knowledge of water condition.

Model validation

Blue whiting along western european shelf edge: Ådlandsvik et al. (2001).

Eggs were spawned at 600m depth well below the depth of wind-induced turbulence. This example provided a validation of the biological part of the model, i.e., the switch between Stokes' law and Dalavalle's parametrisation depending on the Reynolds number to estimate the ascent velocity of the egg. Ådlandsvik et al. (2001) provided *in situ* egg distributions as well as egg density measurements with the density-gradient column of Coombs (1981). The egg diameter was 1.08 mm, constant during all egg stages. The egg density increased with egg developmental time. The model run

was started from an initial spawning depth (initial egg density peak at 380-400 m) and transient solutions were estimated for the different egg stages depending on the stage durations reported (Table 6). The model reproduced well the sampled distributions (Fig. 6) thus cross-validating the parametrisation of the egg vertical velocity as well as the egg density measurements.

Anchovy on the French shelf of the bay of Biscay in spring: Motos and Coombs (2000)

Motos and Coombs (2000) reported *in situ* anchovy egg distributions sampled in 1996 on the Biscay French shelf. When the water column was stratified eggs were confined mainly to the upper layer with a surface peak. In areas under the influence of the river plumes where haline and thermal stratification were present, a sub-surface peak in egg abundance was observed close to the pycnocline. At each station the following information was available: position and date, temperature and salinity profiles and wind speed. Tide was deduced from station position and date. Egg density and diameter were not available in Motos and Coombs (2000). Density was adjusted to produce best fit between modelled and sampled distributions. Egg diameter used was that given by Coombs et al. (2004).

Station 9 (28 May 1996) was selected because it showed important thermal and haline stratification, light wind condition and a sub-surface peak in the egg concentration at the pycnocline at 7 m depth (Table 7, Fig.7). The model reproduced the sampled distribution (Fig. 7). Station 10 (28 May 1996) was also selected because it had a less pronounced gradient in temperature and salinity, greater wind condition and showed a surface peak in the egg distribution (Table 7, Fig. 7). The model also reproduced the sampled distribution (Fig. 7). The egg density values estimated independently for stations 9 and 10 were similar (Table 7), thus validating the model. Depending on the hydrological structure and the egg density, the model was able to reproduce the observed sub-surface or surface peaks in the egg distribution.

Boyra et al. (2003) report anchovy egg density measurements performed in 2001 with the density-gradient column of Coombs (1981) using eggs collected close to the Spanish coast. The average value in 2001 was 23.26 (sigma-t) with a standard error of 0.63 (sigma-t). It is noteworthy that the 2001 egg density was too low to allow for the adjustment of the egg distributions sampled in 1996. The alternative solution was to derive egg density values for 1996 knowing the sampled egg distributions in 1996 and compare these to the 2001 density value. The egg density was 25.83 (sigma-t) according to our model in 1996, indicating the possibility of inter-annual significant variation in egg density.

Sardine on the French shelf of the bay of Biscay in spring: Coombs et al. (2004)

Coombs et al. (2004) report *in situ* sardine and anchovy egg distributions sampled in 2000 on the Biscay French shelf. Egg distributions were similar to that observed in 1996 for anchovy. Similarly, at each station the following information was available in the article: position and date, temperature and salinity profiles and egg diameter. Tide was deduced from station position and date. Wind was taken from the lighthouse at Chassiron which was the closest to the sampling stations. Again, egg density

was not available in the article and was adjusted to produce best fit between modelled and sampled distributions.

Station 29 (18 May 2000) was selected for sardine eggs because it showed an important thermal and haline stratification, moderate wind condition and a sub-surface peak in the egg concentration at the pycnocline at 7 m depth. Again, the model reproduced the sampled distribution (Table 7, Fig. 8). The model estimated egg density was 24.5 (sigma-t), a value in agreement with the range of values experimentally measured by Coombs et al. (1985) in 1982 in the English Channel (24-27 sigma-t) but significantly greater than that measured by Boyra et al. (2003) in 2001 in southern Biscay (23.4 sigma-t, std.error 0.44). The question of potential significant variation in egg density is therefore also raised for sardine.

Sardine off Plymouth in summer and autumn: Coombs et al. (1985)

Coombs et al. (1985) reported *in situ* sardine and sprat egg distributions sampled in 1982 off Plymouth in the English Channel, together with egg density measurements performed with the density-gradient column of Coombs (1981). At each station the following information was available: position and date, and temperature and salinity profiles. The hydrological structure showed a thermal stratification in summer while in autumn the density profile was uniform. Tide was deduced from station position and date. Wind on the sampling date was taken from the lighthouse of La Hague which was the closest to the sampling station available to us. The egg diameter was not given and we used the value of 1.64 mm reported in Boyra et al. (2003).

Station 8 (7 July 1982) and station 11 (6 October 1982) were selected because of the difference in hydological and biological structures. In July, in the presence of thermal stratification, the eggs were confined to the first 15 m with a surface peak while in October the egg distribution was less confined and homogeneous in the first 35 m. The model reproduced the sampled distributions in both cases (Table 8, Fig. 9). The model fitted density values (25.4 and 25.5 sigma-t) were in the range of values given in Coombs et al. (1985) (24-27 and 22-26 sigma-t), thus validating the model.

Sprat off Plymouth in spring: Coombs et al. (1985)

Station 4 (9 June 1982) showed thermal stratification and a sub-surface peak in the egg distribution at 20 m depth, allowing us to further validate the model with different egg parameters than previously. The egg diameter was not available and we used the value of 0.9 mm reported in Russel (1976). Again, the model reproduced the sampled distribution (Table 8, Fig. 10). The model fitted egg density was 26.5 (sigma-t) which was in the range of experimental values measured in Coombs et al. (1985) (23-26.5 sigma-t), thus validating the model.

CONCLUSION AND DISCUSSION

Model structure and validation

Because of the dynamic numerical modelling and the turbulence closure scheme, it was possible to reproduce the mixing conditions of a stratified water column in the presence of complex halocline and/or thermocline, under wind and/or tide induced turbulence. These conditions, regularly encountered in spring in the Bay of Biscay French shelf, are typical of shelf seas under tidal and river run-off influences. The model developed here is adapted for such conditions and represents a novel tool for modelling fish egg vertical distributions in shelf seas. The bio-physical coupling through the parametrisation of the egg vertical velocity allowed us to reproduce the different types of egg vertical distributions encountered in survey data for different species (sardine, sprat, anchovy and blue-whiting): (i) confinement in the upper layers above the pycnocline with a surface peak or homogeneous distribution in the upper layer; (ii) sub-surface maximum near the pycnocline; (iii) deep maximum below the pycnocline. It is noteworthy that the present dynamic numerical modelling was able to reproduce sub-surface maxima in the egg distribution, a feature that Boyra et al. (2003) had difficulties reproducing using the analytical model of Sundby (1983). The validation exercise required a list of parameters (sampling position and date, temperature and salinity profiles, wind, egg diameter and density) which were not always collected together with the sampling of egg vertical distributions. It is advised that future studies collect the full set of information, if *in situ* vertical distributions are to be fully used for validation purposes.

Model sensitivity

Wind controlled the vertical egg distribution allowing for a sub-surface maximum to occur or homogenising the distribution. Tide was also an important forcing parameter in shallow waters (depth smaller than 50 m), with a capacity to also homogenise the egg distribution. Model results were sensitive to variations in egg density, determining the vertical position of the egg maximum. The egg concentration in the surface layer (0-5 m) was sensitive to variations in all input parameters, making fine scale monitoring of wind and egg density of primary importance if underway 3 m depth CUFES samples are to be converted to vertically integrated egg abundance using the vertical model. The model could be used as an assessment tool for that purpose.

Model limitation

The model could also be used as a tool to investigate biological processes that are not well understood at present. With the numerical model now available which is adapted to shelf sea processes (tide, wind, haline and thermal stratification), model limitation is thought to reside in biological knowledge more than in the model parametrisation. Variability in the egg parameters (size, density) at each station was not taken into account here. It is potentially feasible to incorporate this variability in

the coding but this would require knowledge on the probability distributions of egg diameter and density as well as the correlation between them. It is expected that taking into account the within station egg variability would result in smoothing the model steady-state profile without changing its shape. The comparison between the within station variability with the spatial and inter-annual variability in the average egg parameters would identify the major source of overall variability. It is anticipated (see below) that the within station variability in egg density is smaller than the spatial and inter-annual variability. Variability in egg parameters at different scales in not well known, making modelled distributions uncertain. Another point is the dependence of the egg distribution on the initial spawning depth. The characteristic time is a parameter that gives insight into the subject. On only one occasion (Table 9: sardine at station 12 on 29 May 1996), was the characteristic time (12.26 days) greater than the egg life span (a few days only). This happened when both egg velocity and mixing were small (small difference between egg and sea water density, low wind and tide conditions). The *in situ* egg distribution was then expected to be dependent on the initial spawning depth. Sardine at this station was omitted from the present study. The model could serve to explore the dependence of the egg distribution to different spawning strategies.

Use of the model with CUFES 3m depth samples

Values obtained for the characteristic time were close to one day for anchovy and sardine eggs when their life span was three to four days. Therefore it seems reasonable to use the vertical model for estimating an indicative egg abundance for all stages pooled. When CUFES egg samples are collected together with acoustic records of the spawning fish, such a model-based egg abundance estimate could be useful for validating acoustic records. But if the vertical model and CUFES samples are to be used for egg production methods, it seems that spawning depth needs to be resolved, making survey design more complex. Egg production methods are based on the estimation of a mortality curve between egg stages and thus require an estimate of egg abundance at stage. Adequate sampling of young egg stages by CUFES depends on spawning depth. Also, it can be anticipated that stage duration for young egg stages will often be shorter (a few hours) than the characteristic time (one day) and thus vertical modelling for these stages will require spawning depth as initial condition.

Variation in egg density

The validation exercise highlighted significant variation in egg density between years, making the use of density measurements problematic when performed in other conditions than that of the sampled vertical distributions. When egg density was measured in the conditions in which the egg distribution was sampled, e.g., blue-whiting (Ådlandsvik et al., 2001) or sardine and sprat (Coombs et al., 1985), values estimated with the model agreed with those measured. In contrast for anchovy and sardine in Biscay, measurements performed in 2001 (Boyra et al., 2003) were not in agreement with densities

estimated when modelling the vertical distributions sampled in 1996 and 2000 (Motos and Coombs, 2000; Coombs et al., 2004).

Differences in temperature when measuring egg density are thought to play a minor role in explaining egg density variation because egg thermal expansion is reported to be small (0.01 sigma-t per °C, Coombs et al., 1985) in comparison to the range of egg density variation (1.5 to 2 sigma-t) observed. It is noteworthy that in spring 2001 in Biscay, surface salinity was very low over the entire shelf (31.17) due to very large river discharges in that year in comparison to 1996 (34.64) and 2000 (34.58). Egg density has been reported to vary in relation with sea water density in the Baltic (e.g., Nissling et al., 1996; Solemdal, 1971) as well as seasonally in the English Channel (Coombs et al., 1985). In the case of sardine, sprat and anchovy, individual egg density is constant throughout the egg life span from fertilisation to just before hatching (Coombs et al., 1985; Coombs et al., 2004). The egg density is determined in the ovary during the process of oocyte hydration prior to the ovulation. Craik and Harvey (1987) describe how the hydration is triggered by the proteolysis of the yolk proteins generating free amino-acids that increase the osmolarity of the oocyte and consequently generate influx of water in the oocyte from the ovarian fluid. The mechanism could be responsible for adapting the egg to the ambient sea water density. We hypothesise that such a density adaptation mechanism during oocyte hydration could explain the inter-annual density variation found in Biscay for both anchovy and sardine: the egg density would vary with ambient sea water density via the adult fish ovarian osmolarity and consequently the individual egg density would vary according to the particular hydrographic condition during spawing. To confirm this possibility, the model was used to simulate a greater number of vertical distributions and the egg density was adjusted for the model to best fit the sampled vertical distributions (Table 9). Density values of the different species (sardine, sprat and anchovy) varied in coherence with each other, meaning that there was a similar process across species adapting the egg density. The model-based estimated egg densities were then plotted against ambient sea water surface density (0-5 m) showing a clear relationship (Fig. 11). As a consequence, it is advised that egg density be considered a variable parameter to be monitored during fisheries surveys together with the hydrological structure. Understanding ecological factors determining variation in egg density is a key to reliable modelling of vertical distributions of fish eggs.

ACKNOWLEDGEMENTS

This work was financed by a post-doctoral fellowship of IFREMER. The work contributed to the project FOREVAR affiliated to GLOBEC, a module of the French program for fisheries ecology integrated research in the Bay of Biscay. Referees and editor are thanked for their constructive comments.

REFERENCES

Ådlandsvik, B., Coombs, S., Sundby, S. and Temple, G. (2001) Buoyancy and vertical distribution of eggs and larvae of blue whiting (*Micromesistius poutassou*): observations and modelling. *Fish. Res.* **50**: 59-72.

Boyra, G., Rueda, L., Coombs, S., Sundby, S., Ådlandsvik, B., Santos, M. and Uriarte, A. (2003) Modelling the vertical distribution of eggs of anchovy (engraulis encrasicolus) and sardine (Sardina pilchardus). *Fish. Oceanogr.* **12**(4/5): 381-395.

Checkley, D., Ortner, P., Settle, L. and Cummings, S. (1997) A continuous underway fish egg sampler. *Fish. Oceanogr.* **6**: 58-73.

Checkley, D., Hunter, R., Motos, L. and van Der Lingen, C. (2000) Report of a workshop on the use of the continuous underway fish egg sampler CUFES for mapping and spawning habitats of pelagic fish. *GLOBEC Rep*. No. **14**: 65pp.

Conway, D., Coombs, S. and Smith, C. (1997) Vertical distribution of fish eggs and larvae in the Irish Sea and southern North Sea. *ICES J. Mar. Sci* **54**: 136-147.

Coombs, S. (1981) A density-gradient column for determining the specific gravity of fish eggs with particular reference to eggs of mackerel *Scomber scombrus*. *Mar. Biol.* **63**: 101-106.

Coombs, S., Boyra, G., Rueda, L., Uriarte, A., Santos, M., Conway, D. and Halliday, N. (2004) Buoyancy measurements and vertical distribution of eggs of sardine (*Sardina pilchardus*) and anchovy (*Engraulis encrasicolus*). *Mar. Biol.* **145**: 959-970.

Coombs, S., Fosh, C. and Keen, M. (1985) The buoyancy and vertical distribution of eggs of sprat (*Sprattus sprattus*) and pilchard (*Sardina pilchardus*). *J. Mar. Biol. Assoc. UK* **65**: 461-474.

Coombs, S., Morgan, D. and Halliday, N. (2001) Seasonal and ontogenetic changes in the vertical distribution of eggs and larvae of mackerel (*Scomber scombrus* L.) and horse mackerel (*Trachurus trachurus* L.). *Fish. Res.* **50**: 27-40.

Clift, R., Grau, R. and Weber, M. (1978) *Bubbles drops and particles*. Academic Press, New York.

Craik, J. and Harvey, S. (1987) The causes of buoyancy in eggs of marine teleosts. *J. Mar. Biol. Assoc. UK* **67**: 169-182.

Dalavalle, J. (1948) Dynamics of small particles. Pp. 14-40 (Chapter 2) In: *Micromeristics: the technology of fine particles.* Pitman Publishing Corporation, New York.

Denny, M. (1993) *Air and water: the biology and physics of life's media*. Princeton University Press, Princeton.

Heath, M., Brander, K., Munk, P. and Rankine, P. (1991) Vertical distributions of autumn spawned larval herring (*Clupea harengus* L.) in the North Sea. *Cont. Shelf Res.* **11**(12): 1425-1452.

Hutchinson, G. (1967) The hydrodynamics of the plankton. Pp. 245-305 (Chapter 20) In: *A treatise of limnology*, Vol. II, John Wiley and Sons, New York.

Le Cann, B. (1990) Barotropic tidal dynamics of the Bay of Biscay shelf: observations, numerical modelling and physical interpretation. *Cont. Shelf Res.* **10**(8): 723-758.

Lo, N., Hunter, J. and Charter, R. (2001) Use of a continuous egg sampler for ichthyoplankton surveys: application to the estimation of daily egg production of Pacific sardine (*Sardinops sagax*) off California. *Fish. Bull.* **99**: 554-571.

Luyten, P., Deleersnijder, E., Ozer, J. and Ruddick, K. (1996) Presentation of a family of turbulence closure models for stratified shallow water flows and preliminary application to the Rhine outflow region. *Cont. Shelf Res.* **16**(1): 101-130.

Millero, F. (1974) The physical chemistry of seawater, *Ann. Rev. Earth Planet. Sci.* **2**: 101-150.

Motos, L. and Coombs, S. (2000) Vertical distribution of anchovy eggs and field observations of incubation temperature. *Ozeanografika* **3**: 253-272.

Nissling, A. and Vallin, L. (1996) The ability of cod eggs to maintain neutral buoyancy and the opportunity for survival in fluctuating conditions in the Baltic Sea. *J. Fish Biol.* **48**: 217-227.

Palomera, I. (1991) Vertical distribution of eggs and larvae of *Engraulis encrasicolus* in stratified waters of the western Mediterranean. *Mar. Biol.* **111**: 37-44.

Parada, C., van der Lingen, C., Mullon, C. and Penven, P. (2003) Modelling the effect of buoyancy on the transport of anchovy (Engraulis encrasicolus) eggs from spawning to nursery grounds in the southern Benguela: an IBM approach. *Fish. Oceanogr* **12**: 170-184.

Petitgas, P., Massé, J., Beillois, P., Bourriau, P., Santos, M., Lazure, P. and Planque B. (2002) Estimating *in situ* daily fecundity by coupling CUFES to acoustics during fisheries surveys: exploration of the methods potential on anchovy and sardine in Biscay. *ICES CM 2002/O:3*.

Pingree, R., Mardell, G., Holligan, P., Griffiths, D. and Smithers, J. (1982) Celtic Sea and Armorican current structure and the vertical distributions of temperature and chlorophyll. *Cont. Shelf Res.* **1**(1): 99-116.

Planque, B., Lazure, P. and Jégou, A.-M. (2003) Interannual variability in spring hydrological changes: a method for typological classification and an application to the Bay of Biscay continental shelf. *ICES CM 2003/P:30*.

Solemdal, P. (1971) Prespawning flounders transferred to different salinities and the effects on their eggs. *Vie et Milieu* **1**(Suppl. 22): 409-423.

Stenevik, E., Sundby, S. and Cloete, R. (2001) Influence of buoyancy and vertical distribution of sardine *Sardinops sagax* eggs and larvae on their transport in the northern Benguela ecosystem. *S. Afr. J. Mar. Sci.* **23**: 85-97.

Sundby, S. (1983) A one-dimensional model for the vertical distribution of pelagic fish eggs in the mixed layer. *Deep Sea Res.* **30**(6A): 645-661.

Sundby, S. (1991) Factors affecting the vertical distribution of eggs. *ICES Mar. Sci. Symp.* **192**: 33-38.

Russel, F. (1976) *The eggs and planktonic stages of British marine fishes*. Academic Press, London, 524pp.

Tanaka, Y. (1992) Japanese anchovy egg accumulation at sea surface or pycnocline: observation and model. *J. Oceanogr.* **48**: 461-472.

Westgard, T. (1989) Two models for the vertical distribution of pelagic fish eggs in the turbulent upper layer of the ocean. *Rapp. P.-V. Réun. Const. Int. Explor. Mer* **191**: 195-200.

Williams, R., Collins, N. and Conway, D. (1983) The double LHPR system: a high speed micro- and macroplankton sampler. *Deep-Sea Res.* **30A**: 331-342.

Zeldis, J., Grimes, P. and Ingerson, J. (1995) Ascent rates, vertical distribution and a thermal history model of development of orange roughy, *Hoplostethus atlanticus*, eggs in the water column. *Fish. Bull.* **93**: 373-385.

		Salinity			
		< 30	30 – 32.5	32.5 – 35	> 35
Temperature (°C)	< 10.0	1.477	1.483	1.488	1.495
	10.0 – 12.5	1.369	1.374	1.379	1.385
	12.5 – 15.0	1.282	1.288	1.292	1.298
	15.0 – 17.5	1.196	1.201	1.206	1.211
	17.5 – 20.0	1.125	1.131	1.136	1.145
	20.0 – 22.5	1.055	1.061	1.066	1.070
	22.5 – 25.0	0.998	1.004	1.008	1.013
	> 25.0	0.941	0.946	0.951	0.955

Table 1. Dynamic viscosity μ (10^{-2} g cm^{-1} s^{-1}) of sea water for different ranges of temperature and salinity at normal pressure, after Millero (1974).

	Group 1	Group 2	Group 3	Group 4
CTD Station	F0125	E0372	H0236	F0223
Latitude	47°16’N	45°40’N	44°52’N	45°20’N
Longitude	5°12’W	1°25’W	2°17’W	1°40’W
Date	06 May 2001	24 April 2000	03 June 2003	22 May 2001
Depth (m)	140	25	203	51
Wind ($m\ s^{-1}$)	9	1.2	6	9
Tide ($m\ s^{-1}$)	0.55	0.19	0.12	0.17

Table 2. CTD stations closest to hydrodographic group centres used for the model sensitivity analysis. Group 1: homogeneous density profile; Group 2: haline stratification; Group 3: thermal stratification; Group 4: haline and thermal stratification.

	Decrease	Reference	Increase
Wind ($m\ s^{-1}$)	Half of ref	That at CTD station	Double of ref
Tide ($m\ s^{-1}$)	0.2	0.8	1.3
Anchovy egg diameter (mm)	0.6	0.8	1
Sardine egg diameter (mm)	1.23	1.64	2.05
Anchovy density (sigma-t)	22.63	23.26	23.89
Sardine density (sigma-t)	23.03	23.49	23.94

Table 3. Variation in the input model parameters for the sensitivity analysis. Reference values for wind are that measured at the reference CTD stations (Table 2). Reference values for the egg diameter and density are taken from Coombs et al. (2004) and Boyra et al. (2003). Variations in egg parameters are +/- the standard deviation.

	Decrease	Increase
Impact of wind		
G1	1.99	1.45
G2	5.69	9.67
G3	2.83	2.68
G4	103.28	17.35
Impact of Tide		
G1	0.003	0.009
G2	40.23	1.07
G3	0.002	0.0004
G4	0.0002	0.44
Impact of anchovy diameter		
G1	0.53	0.24
G2	0.92	0.55
G3	0.47	0.20
G4	2.95	2.91
Impact of Sardine diameter		
G1	0.20	0.08
G2	9.86	5.39
G3	0.28	0.13
G4	2.11	1.69
Impact of anchovy density		
G1	0.05	0.08
G2	4.75	488.44
G3	0.06	0.11
G4	15.27	58.384
Impact of sardine density		
G1	0.01	0.02
G2	259.38	603.91
G3	0.03	0.05
G4	19.35	127.19

Table 4. Root mean square difference (RMSD) in the first 50 m between the egg profile of the reference run (RR) and that obtained by varying input model parameters for each hydrological group (Tables 2 and 3). G1: homogeneous density profile; G2: haline stratification; G3: thermal stratification; G4: haline and thermal stratification.

	Decrease %	Increase %
Impact of wind		
G1	65	-56
G2	10	-21
G3	49	-49
G4	-100	108
Impact of Tide		
G1	2	-4
G2	188	-20
G3	1	-1
G4	0	-10
Impact of anchovy diameter		
G1	-34	23
G2	-6	4
G3	-20	13
G4	69	-47
Impact of Sardine diameter		
G1	-13	9
G2	68	-44
G3	-11	8
G4	186	-56
Impact of anchovy density		
G1	10	-13
G2	9	-100
G3	7	-10
G4	148	-90
Impact of sardine density		
G1	3	-4
G2	525	-100
G3	4	-5
G4	388	-98

Table 5. Proportion of eggs in the surface layer (0-5m) relative to the reference run when the input model parameters are decreased or increased for each hydrological condition (Tables 2 and 3). G1: homogeneous density profile; G2: haline stratification; G3: thermal stratification; G4: haline and thermal stratification.

T-S profile	homogeneous
Depth (m)	600
Wind (m s^{-1})	7.5
Tide (m s^{-1})	0
Sea water surface density (sigma-t)	27.26
Egg diameter (mm)	1.08
Egg density	(sigma-t)
Stage 1	27.34
Stage 2	27.83
Stage 3	28.71
Stage 4	29.20
Egg developmental time	(hours from fertilization)
Stage 1	14.4
Stage 2	38.4
Stage 3	64.4
Stage 4	94.9

Table 6. Model parameters for simulating blue whiting egg distributions (Fig. 6) as reported in Ådlandsvik et al. (2001)

	Station 9 28 May 1996	Station 10 28 May 1996	Station 29 18 May 2000
Species	anchovy	anchovy	sardine
Reference	Motos and Coombs (2000)	Motos and Coombs (2000)	Coombs et al. (in press)
T-S profile	Important thermal and haline stratification	Slight thermal and haline stratification	Important thermal and haline stratification
Depth (m)	41	38	33
Latitude	45°33' N	45°22' N	45°43' N
Longitude	1°33' W	1°35' W	1°43' W
Wind ($m\ s^{-1}$)	1.03	5.14	8
Tide ($m\ s^{-1}$)	0.15	0.16	0.27
Sea water surface density	23.53	25.35	23.08
Egg density (sigma-t)	24.79 (adjusted)	24.85 (adjusted)	24.55 (adjusted)
Egg diameter (mm)	0.89	0.89	1.64
Characteristic time (days)	1.28	1.23	0.28

Table 7. Model parameters for simulating egg distributions. The egg density is adjusted to provide the best fit between modelled and observed distributions. Tide is deduced from each station position and date. The egg diameter is that reported by Boyra et al. (2003). Wind speed is taken from the lighthouse of Chassiron on Île de Ré for station 29.

	Station 8 7 July 1982	Station 11 6 October 1982	Station 4 9 June 1982
Species	sardine	sardine	sprat
Reference	Coombs et al. (1985)	Coombs et al. (1985)	Coombs et al. (1985)
T-S profile	Thermal stratification	Homogeneous	Thermal stratification
Depth (m)	50	50	50
Latitude	50°15'N	50°15'N	50°15'N
Longitude	4°13'W	4°13'W	4°13'W
Wind (m s-1)	8.5	8.4	7.4
Tide (m s-1)	0.29	0.38	0.29
Sea water surface density	25.51	25.71	25.64
Egg density (sigma-t)	25.50	25.40	26.48
Egg diameter (mm)	1.64	1.64	0.9
Characteristic time (days)	1.20	0.67	3.34

Table 8. Model parameters for simulating egg distributions. The egg density is that measured at 15°C by Coombs et al. (1985). Tide is deduced from each station position and date. The egg diameter used is that by Coombs et al. (2004) for stations 8 and 11 and by Russel (1976) for station 4. Wind speed is taken from the lighthouse of La Hague.

Station Date	Reference	Surface water density (sigma-t)	Anchovy egg density (sigma-t)	Sardine egg density (sigma-t)	Sprat egg density (sigma-t)s
St 04 9 June 1982	Coombs et al. (1985)	25.7255	-	-	26.48
St 05 16 June 1982	Coombs et al. (1985)	25.5316	-	25.86	26.05
St 08 07 July 1982	Coombs et al. (1985)	25.5336	-	25.505	26
St 11 06 October 1982	Coombs et al. (1985)	25.7147	-	25.4	-
St 06 27 May 1996	Motos et al. (2000)	25.304	25.35	-	-
St 09 28 May 1996	Motos et al. (2000)	24.3351	24.795	-	-
St 10 28 May 1996	Motos et al. (2000)	25.2349	24.85	-	-
St 12 29 May 1996	Motos et al. (2000)	26.3658	26.45	-	-
St 15 09 May 2000	Coombs et al. (2004)	26.1703	26.167	26.15	-
St 29 18 May 2000	Coombs et al. (2004)	23.1224	24.5	24.55	-

Table 9. Model estimated egg densities and sea surface (0-5 m) water density at different stations taken from indicated references and plotted in Figure 11.

LIST OF FIGURES

Figure 9: Vertical distributions of sardine eggs (Coombs et al., 1985) at station 8 (07 July 1982) (top) and station 11 (06 October 1982) (bottom) Continuous line: observed distribution. Dotted line: modelled distribution. Model parameters are in Table 8.

Figure 10: Vertical distribution of sprat eggs (Coombs et al., 1985) at station 4 (09 juin 1982). Continuous line: observed distribution. Dotted line: modelled distribution. Model parameters are in Table 8.

Figure 11: Relationship between the density of ambient sea surface (0-5m) water density and that of the egg density. The egg density was estimated from the model to best fit the sampled vertical distributions (Table 9).

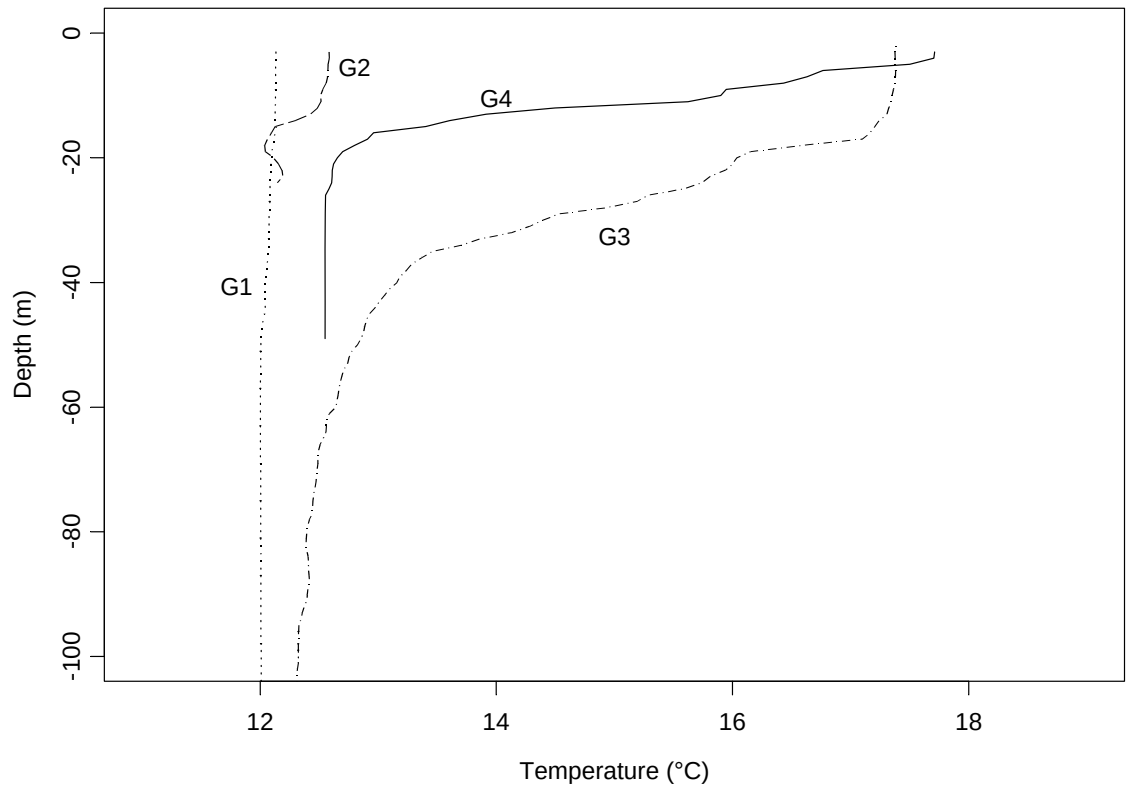
0
-20
-40
-60
-80
-100
Depth (m)
G1
G2
G3
G4
12
14
16
18
Temperature (°C)

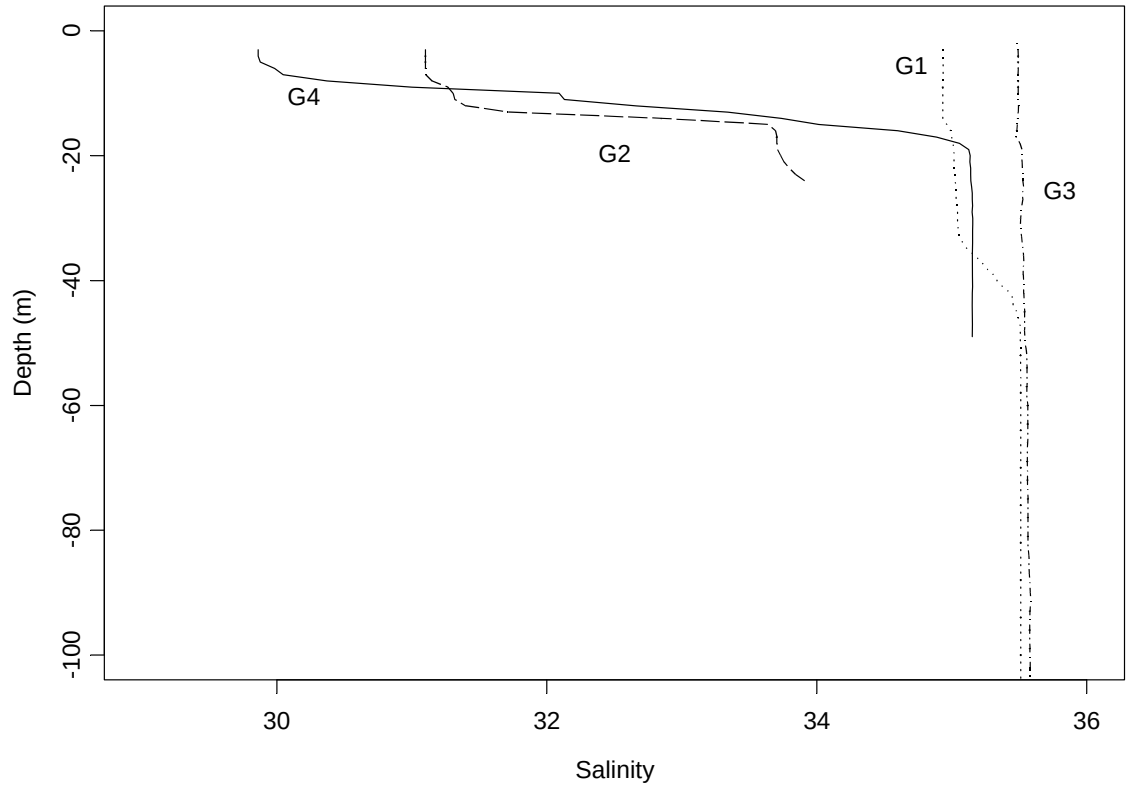
0
-20
-40
-60
-80
-100
Depth (m)
G1
G2
G3
G4
30
32
34
36
Salinity

Figure 1

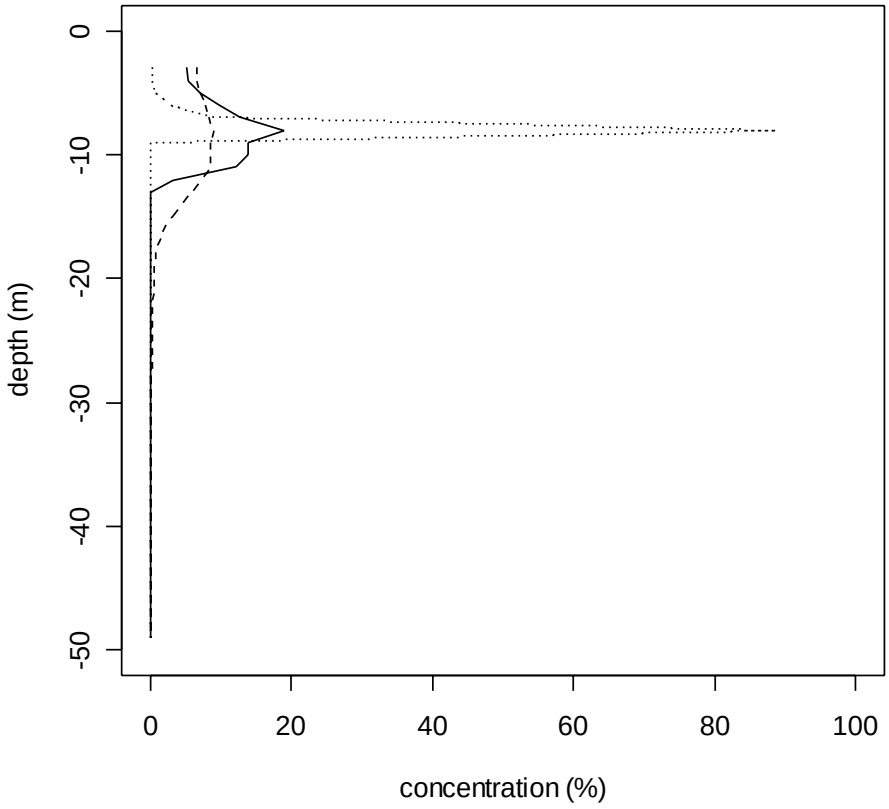
depth (m)
0
-10
-20
-30
-40
-50
0
20
40
60
80
100
concentration (%)

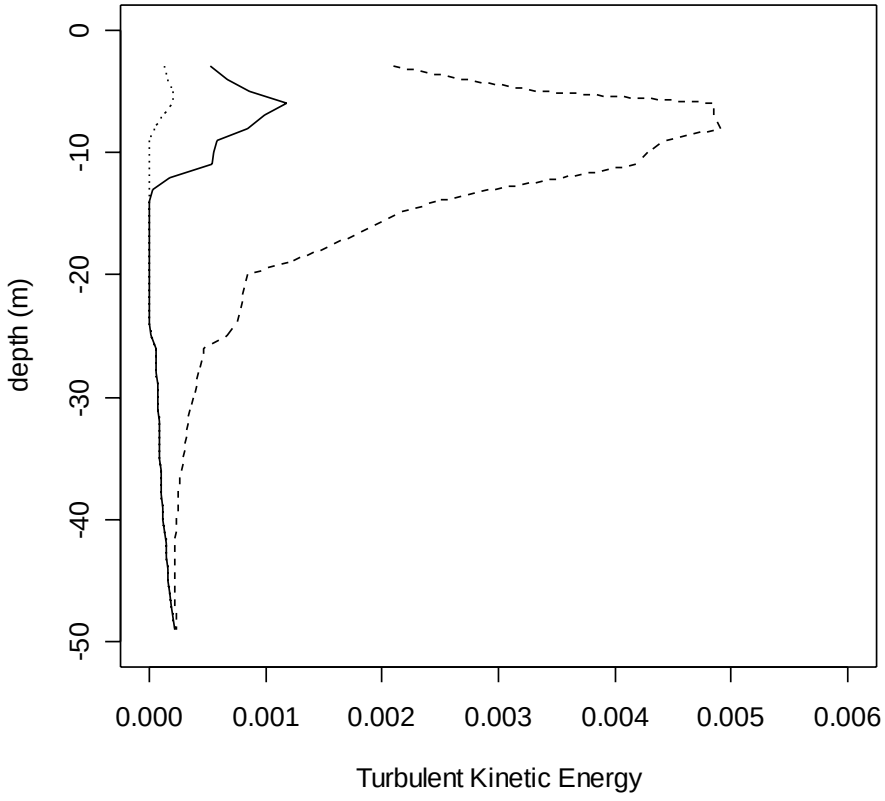
depth (m)
0
-10
-20
-30
-40
-50
0.000
0.001
0.002
0.003
0.004
0.005
0.006
Turbulent Kinetic Energy

Figure 2

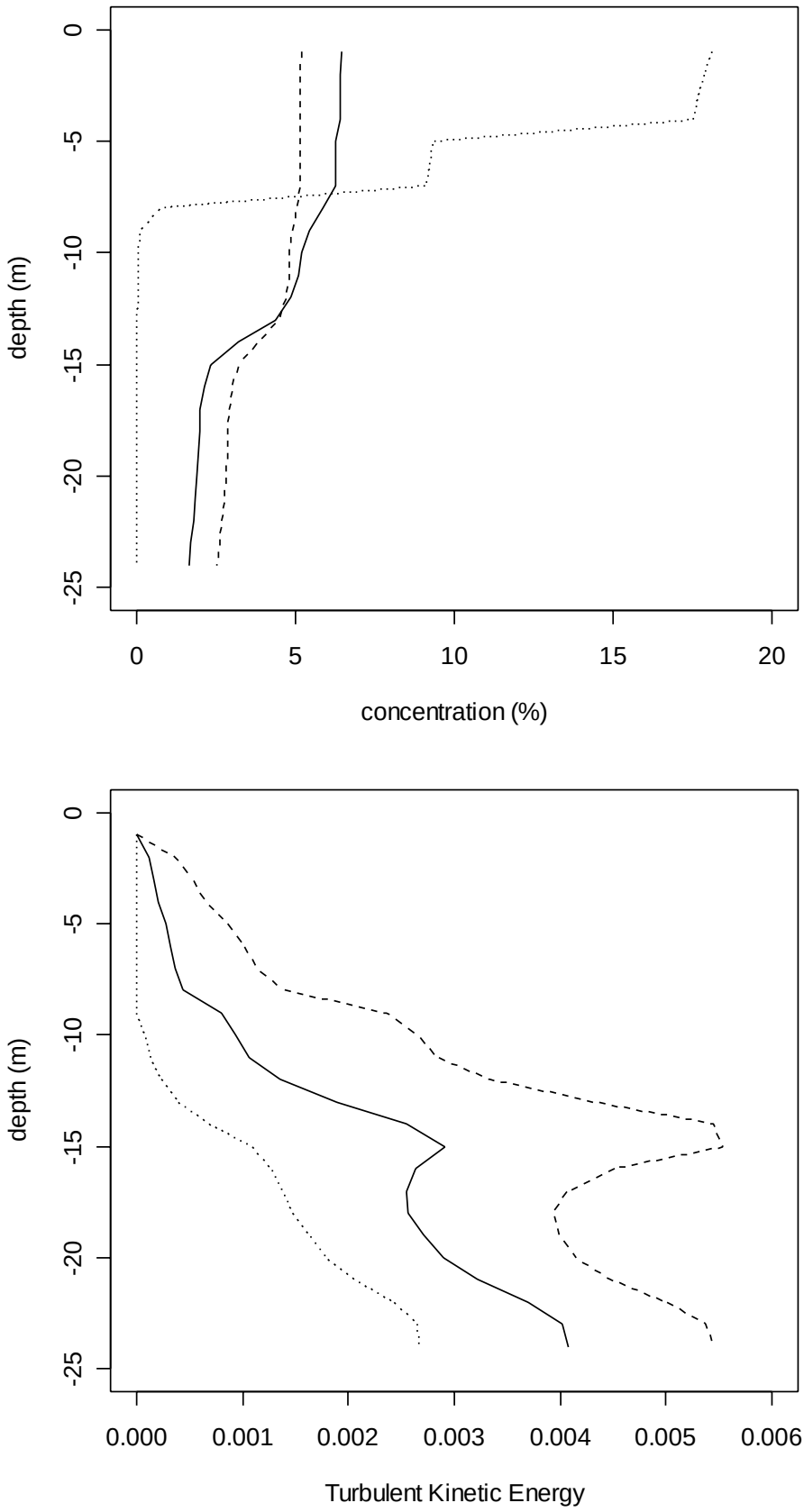
depth (m)
0
-5
-10
-15
-20
-25
0
5
10
15
20
concentration (%)
depth (m)
0
-5
-10
-15
-20
-25
0.000
0.001
0.002
0.003
0.004
0.005
0.006
Turbulent Kinetic Energy

Figure 3

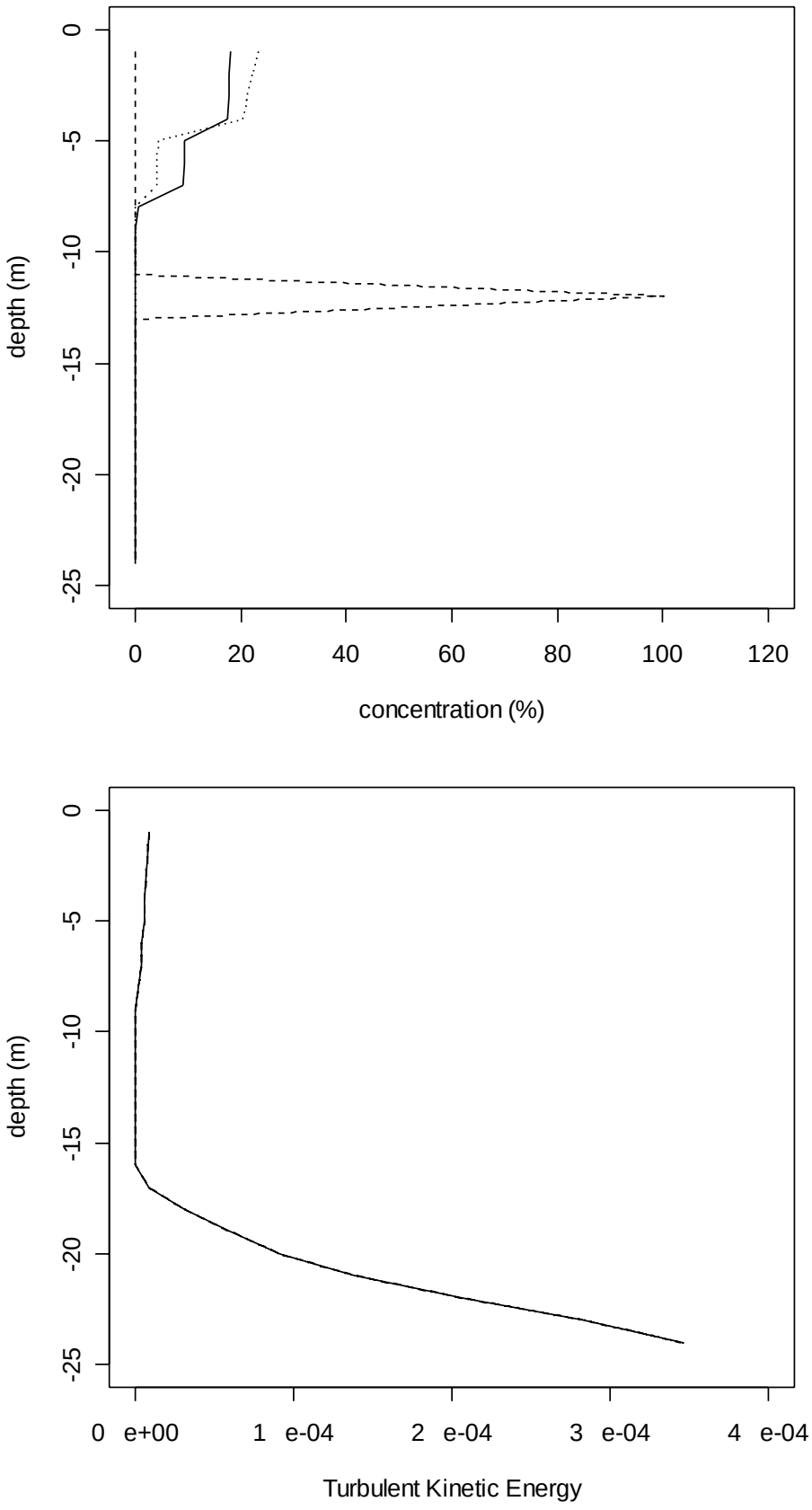
depth (m)
0
-5
-10
-15
-20
-25
0
20
40
60
80
100
120
concentration (%)
depth (m)
0
-5
-10
-15
-20
-25
0 e+00
1 e-04
2 e-04
3 e-04
4 e-04
Turbulent Kinetic Energy

Figure 4

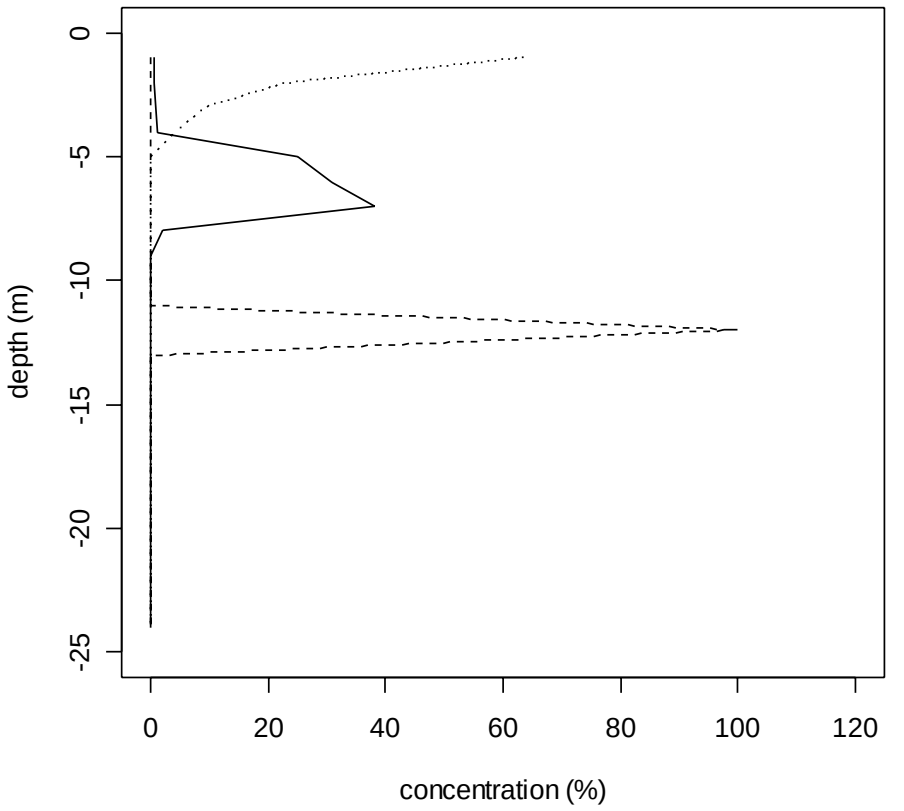
depth (m)
0
-5
-10
-15
-20
-25
0
20
40
60
80
100
120
concentration (%)

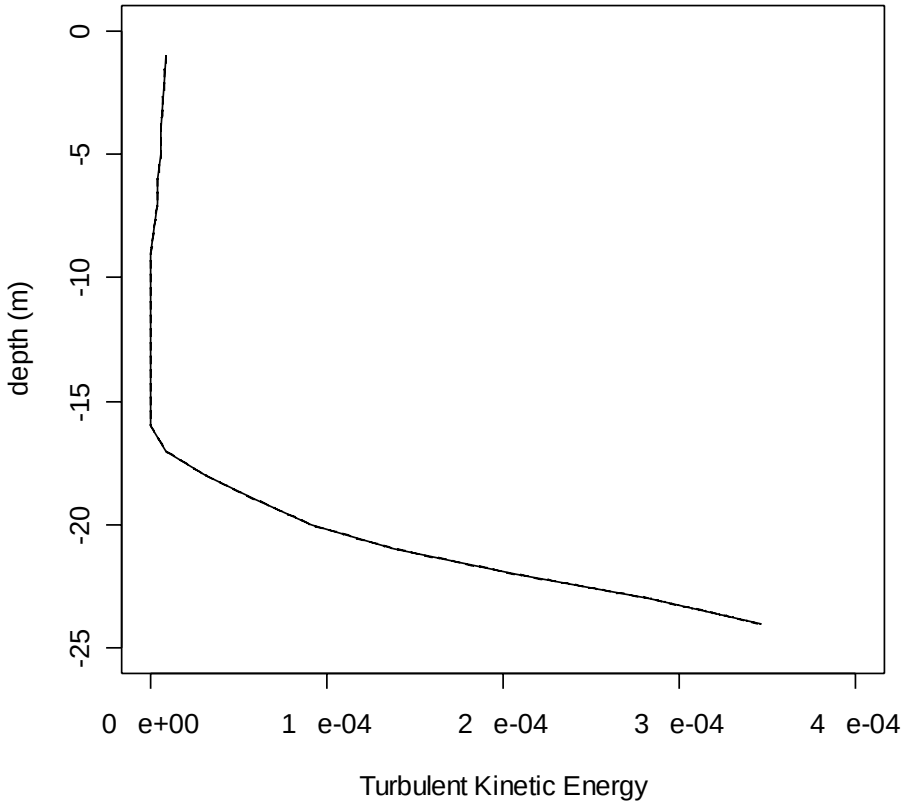
depth (m)
0
-5
-10
-15
-20
-25
0 e+00
1 e-04
2 e-04
3 e-04
4 e-04
Turbulent Kinetic Energy

Figure 5

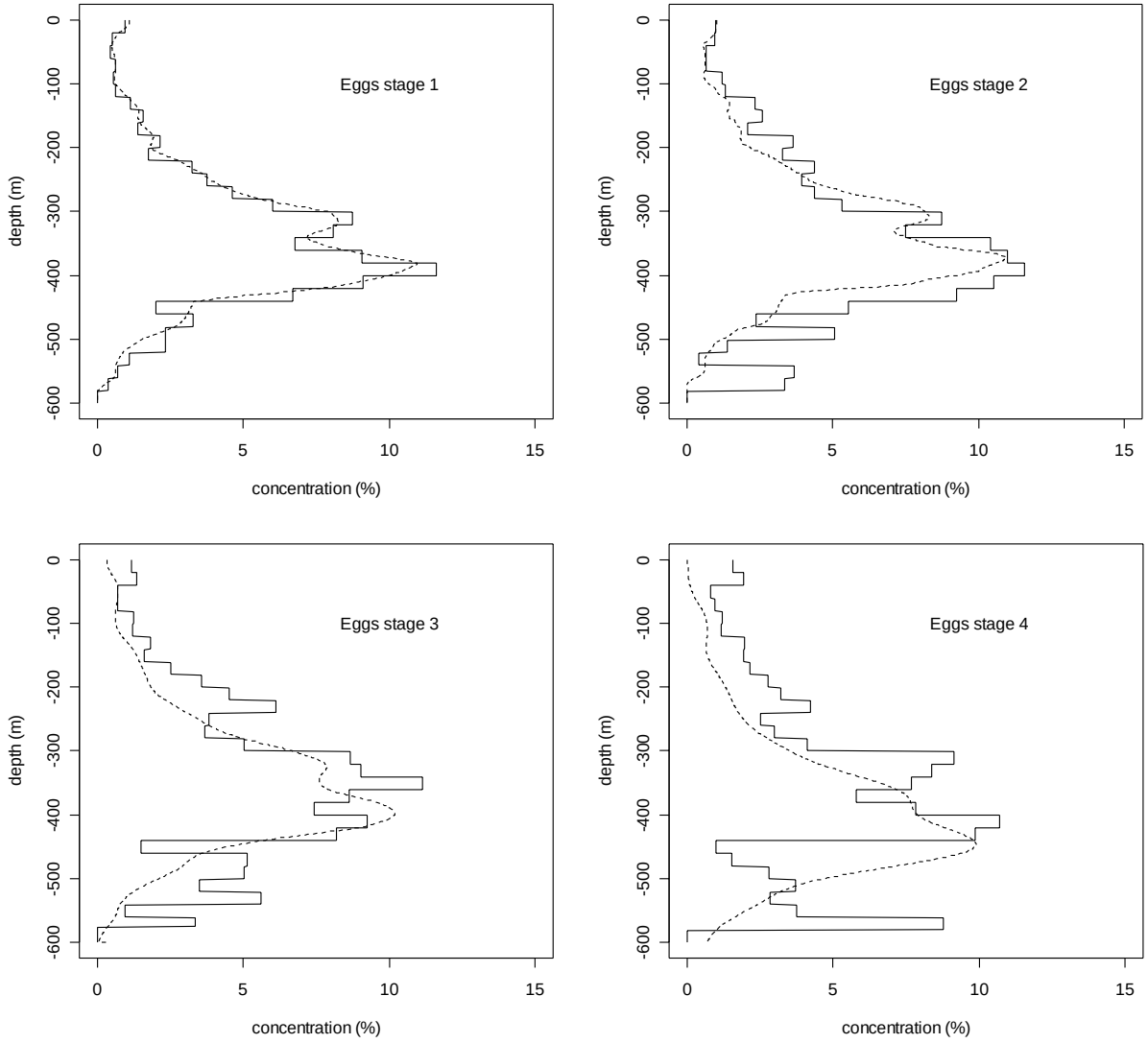
Eggs stage 1
Eggs stage 2
Eggs stage 3
Eggs stage 4
depth (m)
0
-100
-200
-300
-400
-500
-600
0
5
10
15
concentration (%)

Figure 6

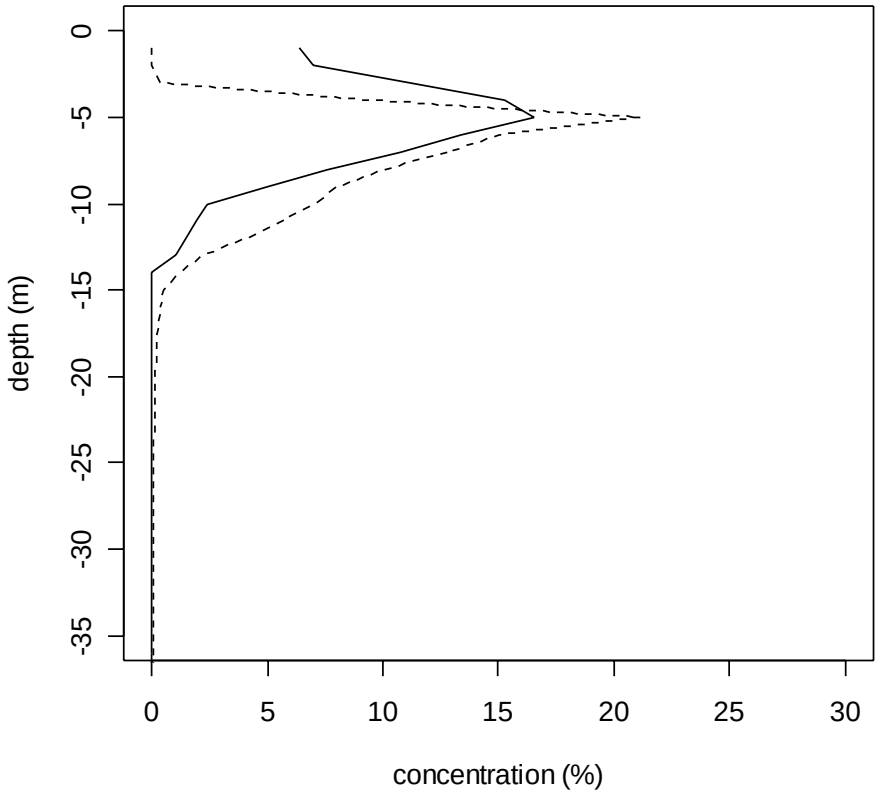
depth (m)
0
-5
-10
-15
-20
-25
-30
-35
0
5
10
15
20
25
30
concentration (%)

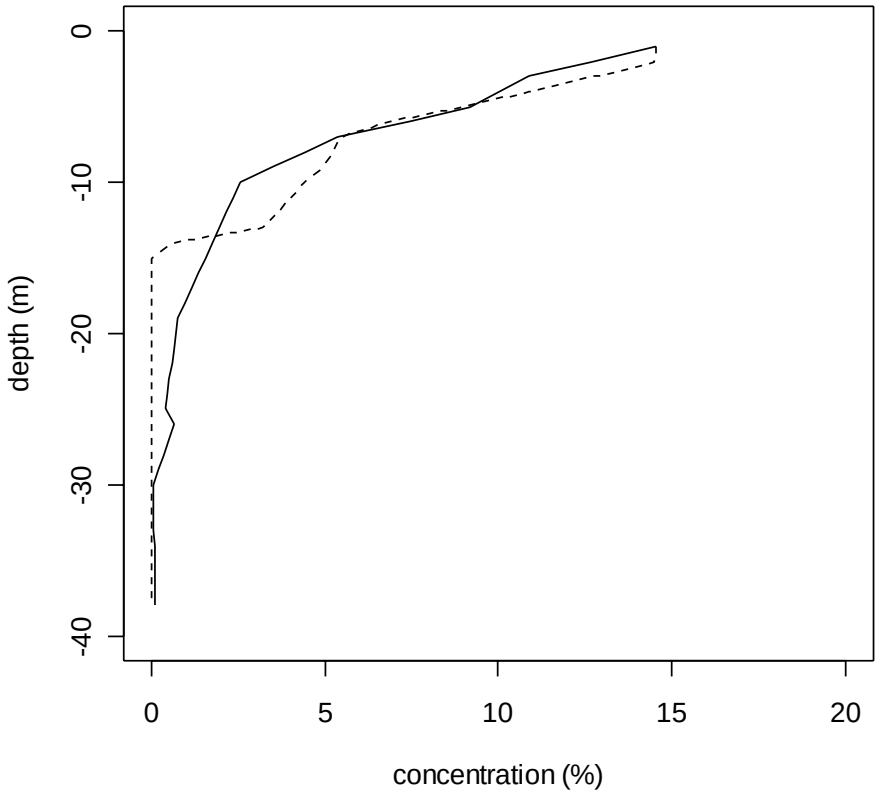
depth (m)
0
-10
-20
-30
-40
0
5
10
15
20
concentration (%)

Figure 7

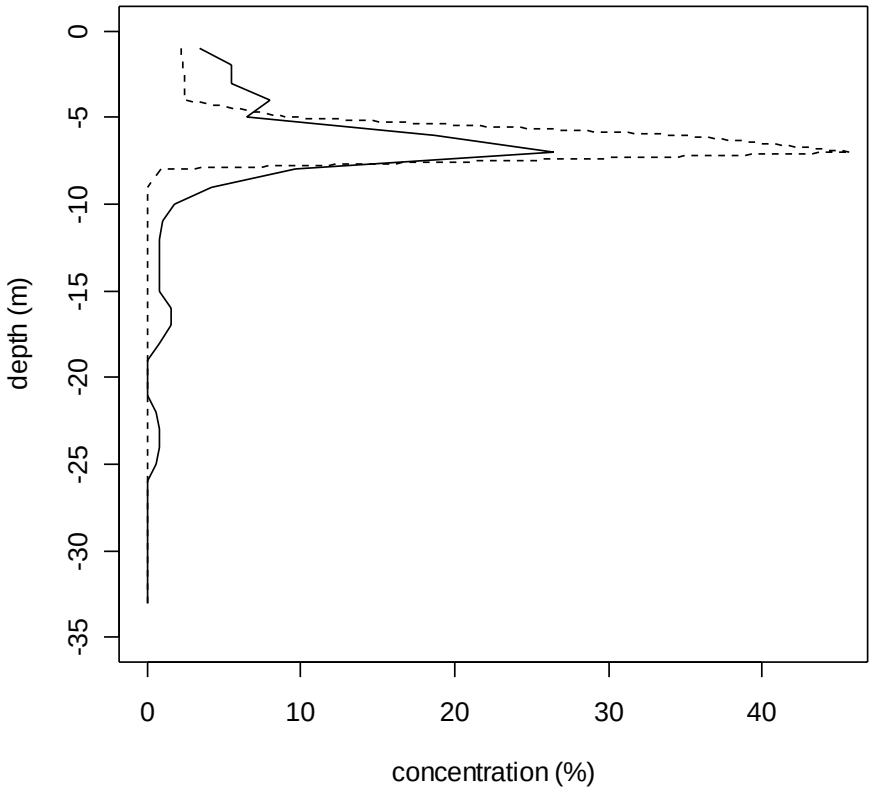

Figure 8

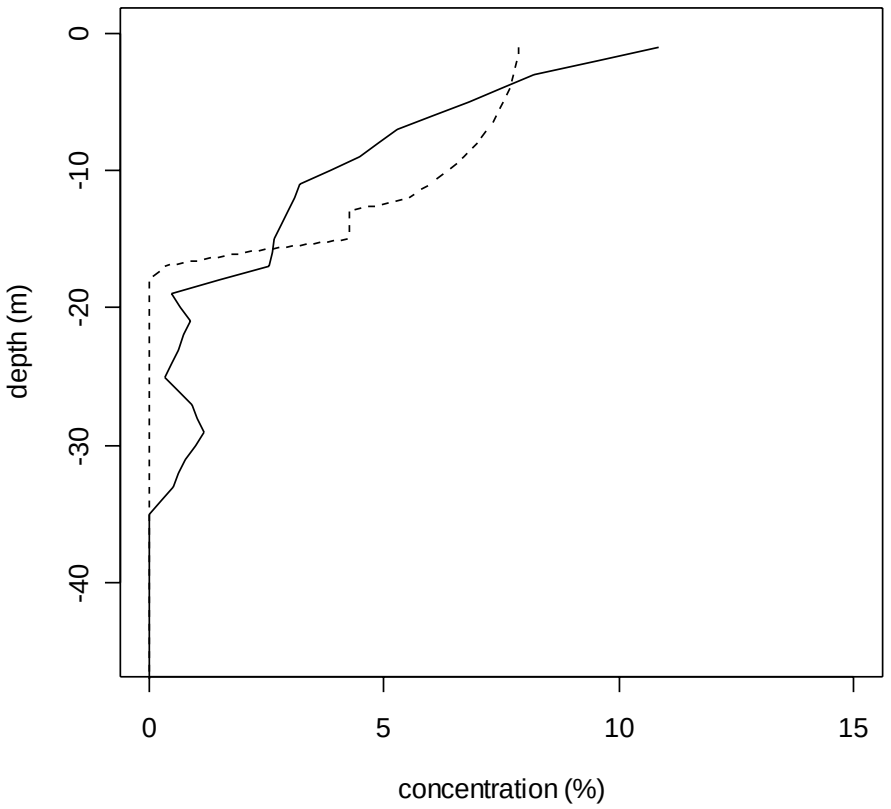
depth (m)
0
-10
-20
-30
-40
0
5
10
15
concentration (%)

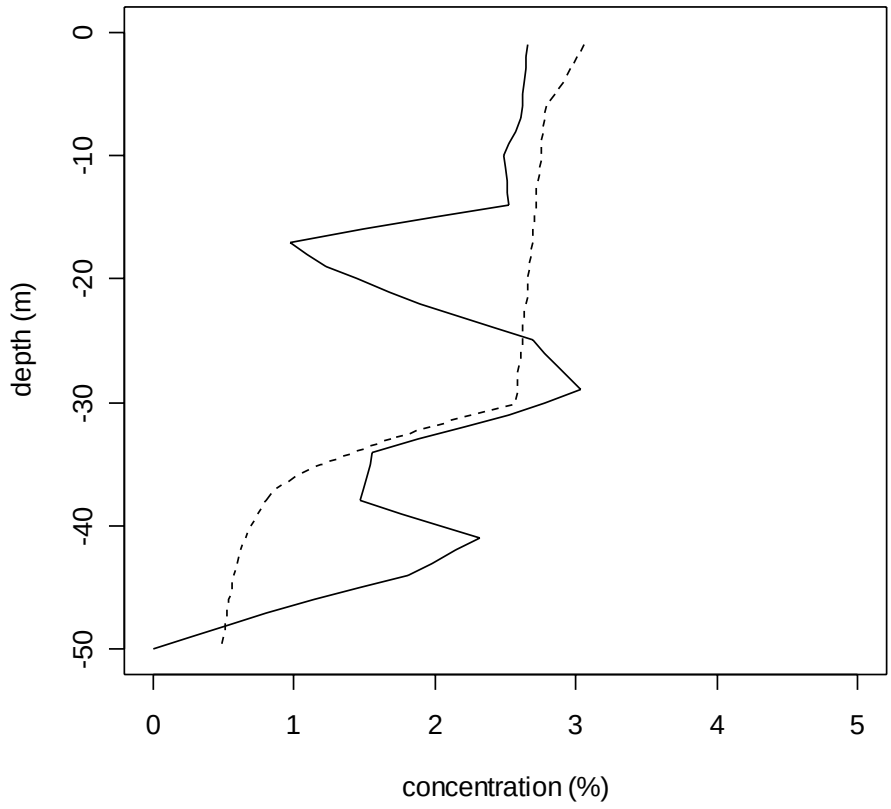
depth (m)
0
-10
-20
-30
-40
-50
0
1
2
3
4
5
concentration (%)

Figure 9

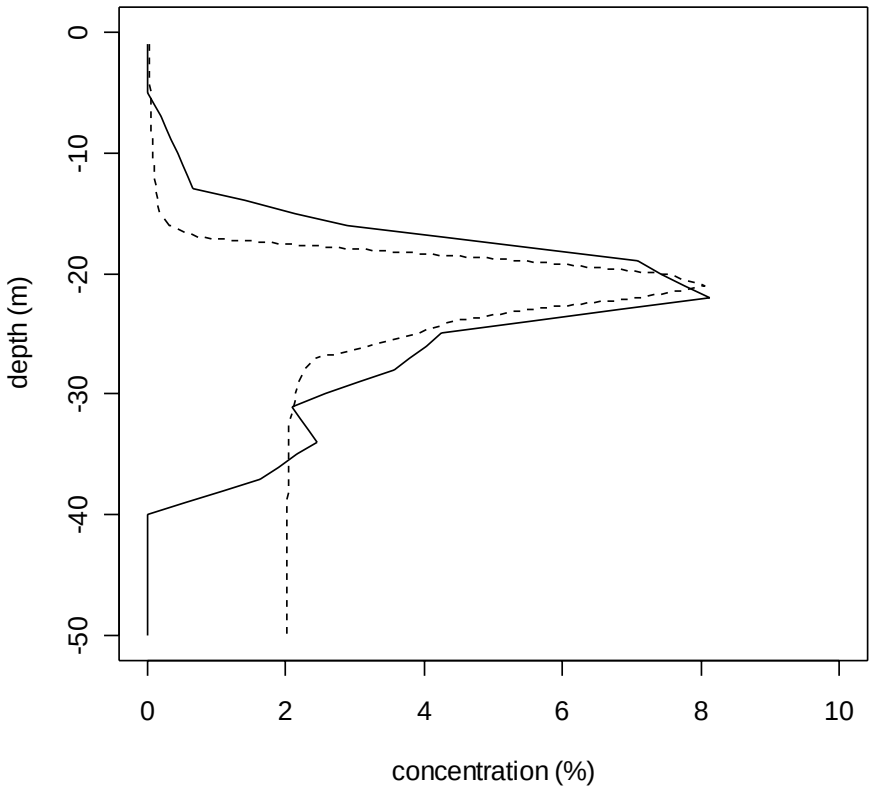

Figure 10

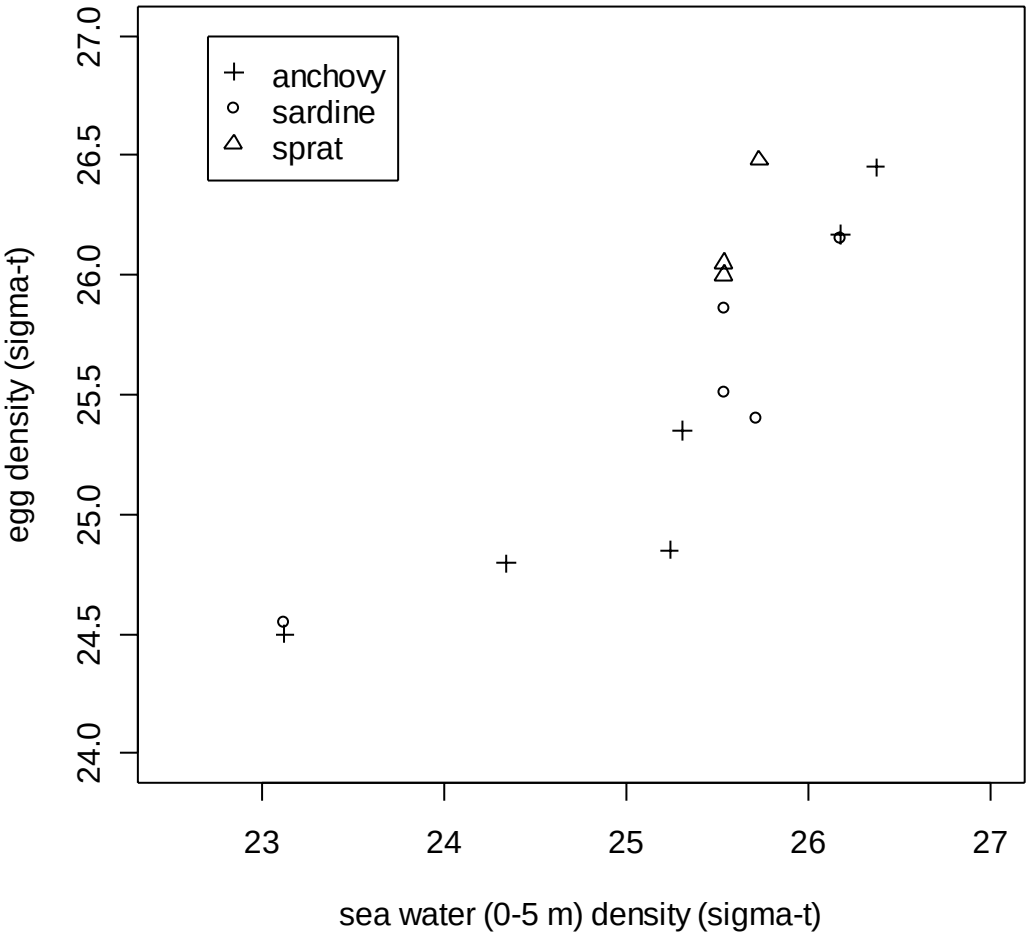
anchovy
sardine
sprat
egg density (sigma-t)
24.0
24.5
25.0
25.5
26.0
26.5
27.0
23
24
25
26
27
sea water (0-5 m) density (sigma-t)

Figure 11